COLLECTOR DESIGN FOR MEASURING HIGH-INTENSITY TIME VARIANT SPRINKLER APPLICATION RATES

B. A. King, R. W. Wall, T. W. Winward, D. L. Bjorneberg

ABSTRACT. *Peak water application rate in relation to soil water infiltration rate and soil surface storage capacity is important in the design of center pivot sprinkler irrigation systems for efficient irrigation and soil erosion control. Measurement of application rates of center pivot irrigation systems has traditionally used tipping bucket rain gauges. Calculation of application rate from tipping bucket rain gauge measurements restricts computed application rate to a discrete multiple of the rain gauge resolution and time interval. This limits the resolution of application rate measurement, especially for time intervals less than 15 min. A collector was designed to measure time variant high-intensity sprinkler application rates under field conditions with greater resolution than a tipping bucket rain gauge. The collector funneled water into a 50-mm (2-in.) diameter tube providing a depth multiplication factor of 18.26:1. The depth of water in the tube was measured with a low pressure piezo-resistive pressure sensor connected to a differential amplifier circuit. Combination of the depth multiplication factor of the collector and differential amplifier circuit provided a collector resolution of 1.4 mm/mV (0.055 in./mV). A data logger was used to record water depth in the collector tube during an irrigation event. A digital differentiating filter was designed and used to reduce the effect of random electrical noise in the sensor output on calculated application rate. The collector was tested in the laboratory and under field conditions simulating center pivot sprinkler irrigation. For a range in application rates from 15 to 200 mm/h (0.7 to 8 in./h) and application depths from 20 to 35 mm (0.8 to 1.4 in.) in the laboratory, the maximum collector error was 2.1 mm/h (0.08 in./h). Collector-measured application rate patterns under field conditions were well-correlated to simulated application rate patterns using radial application rate profiles for the sprinklers tested. Collector-measured peak application rates were not significantly different from those predicted by the Kincaid (2005) model. The collector functioned as designed in field tests and provided an effective and efficient means of measuring high-intensity application rates from center pivot irrigation systems under field conditions.*

Keywords. Sprinkler irrigation, Center pivot, Application rate.

Mechanized irrigation systems such as center pivot and lateral move sprinkler systems have become the irrigation system of choice for much of the United States. These automated sprinkler irrigation systems reduce labor costs compared to surface and set-move sprinkler systems, typically increase water application uniformity and efficiency, and reduce water quality impacts compared to surface irrigation systems. Over 48% of the irrigated area in the United States uses mechanical move sprinkler irrigation systems (USDA, 2009). The main problem associated with center pivot sprinkler irrigation systems continues to be potential runoff

(water redistribution from point of application) due to high application rates along the outer extent of the lateral. Several investigators have discussed the importance of peak application rates in relation to soil water infiltration rates and soil surface storage capacity in the design of center pivot sprinkler irrigation systems (Kincaid et al., 1969; Dillion et al., 1972; Gilley, 1984; DeBoer et al., 1988; Allen, 1990; DeBoer et al., 1992; Wilmes et al., 1993; DeBoer, 2001). Over the past two decades, manufacturers have developed sprinklers that can produce high application uniformity with controlled drop sizes and pattern widths in the range of 14 to 17 m (46 to 56 ft) at pressures less than 138 kPa (20 psi) (Kincaid et al., 2000). Peak application rates under center pivot sprinkler irrigation systems equipped with these sprinklers often exceed soil water infiltration rates. Thus, knowledge of peak application rates is still required in order to design center pivot irrigation systems that minimize the potential for runoff or water redistribution in the field.

Peak application rates can be estimated from sprinkler radial application rate pattern data using computer simulation of sprinkler pattern overlap to calculate a composite application rate pattern. However, the actual application rate pattern will differ due to the stop-start movement of center pivot sprinkler lateral towers, the effect of wind on droplet trajectory, and the presence of pattern interference due to structural elements of the irrigation system and sprinklers. Thus, it is desirable to be able to directly measure sprinkler application rate at time intervals

The authors are **Bradley A. King, ASABE Member Engineer,** Research Agricultural Engineer, USDA ARS NWISRL, Kimberly, Idaho; **Richard W. Wall,** Professor, Department of Electrical and Computer Engineering, University of Idaho, Moscow, Idaho; **Troy W. Winward,** Hydrologic Technician, and **David L. Bjorneberg, ASABE Member Engineer,** Supervisory Research Agricultural Engineer, USDA ARS NWISRL, Kimberly Idaho. **Corresponding author:** Bradley A. King, USDA ARS NWISRL, 3793 N. 3600 E., Kimberly, ID 83341-5076; phone: 208-423-5061; fax: 208-423-6555; e-mail: brad.king@ars.usda.gov.

of 1-min duration or less to evaluate these effects on peak application rates and validate computer simulation of peak application rate, runoff, and erosion.

Tipping bucket rain gauges traditionally have been used to measure and record cumulative sprinkler application depth with time and calculate application rate from the cumulative depth curve. This procedure has some deficiencies due to the mechanical nature of the tipping bucket rain gauge (e.g., Scherer and Weigel, 1995). Commonly the number of tips of known bucket volume (equivalent depth) during a specified time interval is recorded along with time. Calculation of application rate as the time derivative of cumulative application depth will always be a multiple of the bucket volume divided by time interval. For example, if the time interval is 1 min and the bucket volume is equivalent to a depth of 0.254 mm (0.01 in.), then the 1-min application rate will always be a discrete multiple of 15.24 mm/h (0.6 in./h). This binning effect is time interval dependent and becomes insignificant for time intervals greater than 15 min (Habib et al., 2001). The mechanical nature of the tipping bucket rain gauge requires dynamic calibration for accurate measurement at precipitation rates greater than 50 mm/h (2 in./h) (Humphrey et al., 1997). Another typical problem that affects calculation of application rate is that the tipping bucket rain gauge cannot provide start and stop times of an application event. One approach to alleviate the problem of binning is to fit a continuous function to the cumulative application depth data and then differentiate the continuous function. The performance of this approach depends upon how well the selected function fits the cumulative depth data. Another approach is to use a cubic spline curve fit and numerically differentiate the cubic spline function (Sadler and Busscher, 1989; Wang et al., 2008). The physical limitations associated with a mechanical tipping bucket rain gauge limits its use for measuring peak water application rates under center pivot sprinkler irrigation. New methods of data analysis or different rain gauge designs are needed to accurately measure peak application rates.

The objective of this work was to develop and test an inexpensive collector for measuring peak application rates of 1-min duration or less under center pivot sprinkler irrigation that eliminates the binning effect associated with tipping bucket rain gauges.

DESIGN CONSIDERATIONS

The peak application rate to be measured is the maximum point on the application rate profile as a center pivot sprinkler irrigation system passes over a fixed location. Higher instantaneous rates can occur for very short periods of time due to concentration of spray streams from several sprinklers, or from grooved non-rotating plates, but these instantaneous rates are difficult to quantify and are not of interest here. Based on expected field conditions, the design requirements developed for a collector to measure peak application rate were:
- Time resolution of 1 min or less.
- Measurement range of 0 to 200 mm/h (0 to 8 in./h).
- Measurement resolution 2.5 mm/h (0.1 in./h).
- Constructed of readily available components.
- Analog output for data logging.

The fundamental approach was to indirectly measure application rate by differentiating cumulative application depth measurements according to:

$$AR(t) = \frac{d(D(t))}{dt} \tag{1}$$

where $AR(t)$ [mm/h (in./h)] is the application rate and $D(t)$ [mm (in.)] is measured application depth at time (t). The last two design requirements limited the sensing approach that could be employed to measure and record cumulative application depth. A piezo-resistive pressure sensor was selected as the sensing element to measure cumulative application depth because they are relatively inexpensive, output an analog signal, have relatively good resolution, and are readily available in pressure ranges less than 600-mm H_2O (~24-in. H_2O).

METHODS AND MATERIALS

The collector developed to measure cumulative application depth is shown in figure 1. A 560-mm (22-in.) length of 50-mm (2-in.) diameter PVC pipe was used as the water volume container. A PVC pipe cap was solvent welded to one end of the water volume container. A hole was drilled though the center of the pipe cap and tapped with 6.3-mm (0.25-in.) pipe threads. A plastic tee was screwed into the hole in the PVC pipe cap. Two lengths of clear tubing were attached to each end of the plastic tee. The tubing was fixed along opposite sides of the water volume container using plastic wire ties. One of the tubes was cut to a length such that the open end of the tube was 50 mm (2 in.) shorter than the length of the water volume container. The other clear tube was cut to a length about 150 mm (6 in.) shorter than the length of the water volume container. A piezo-resistive pressure sensor (20 in.-g-mv-mini, All Sensors, Morgan Hill, Calif.) with a measurement range of ±510 mm H_2O (±20 in. H_2O) differential pressure and a ratiometric differential voltage output of ±20 mV at 12-VDC excitation was attached to the end of the shorter nylon tube using a plastic reducer and short length of 3-mm (0.125-in.) diameter tubing. The piezo-resistive pressure sensor was housed in a splash proof aluminum enclosure which was also fixed to the side of the water volume container using plastic wire ties. A funnel collector from a tipping bucket rain gauge measuring 219 mm (8.625 in) in diameter was used to collect and funnel water into the water volume container. The diameter ratio of the funnel collector to the water volume container provided a depth ratio of 18.26:1. Thus, a 25.4-mm (1-in.) application depth of water results in a water depth of 464 mm (18.26 in.) in the water volume collector. The pressure sensor had a nominal output resolution of 25.4-mm H_2O/mV (1-in. H_2O/mV), which resulted in a 1.4-mm/mV (.055-in./mV) resolution due to the 18.26:1 depth ratio. A three-legged metal stand was clamped to the water volume container to support vertical installation of the collector in the field. A flexible graduated rule was glued to the outside of the water volume container to provide an easy means to manually record the depth of water in the container based on the height of water in the open-ended clear nylon tube. The graduated rule was referenced from the bottom of the water volume container. The height of the water in the water
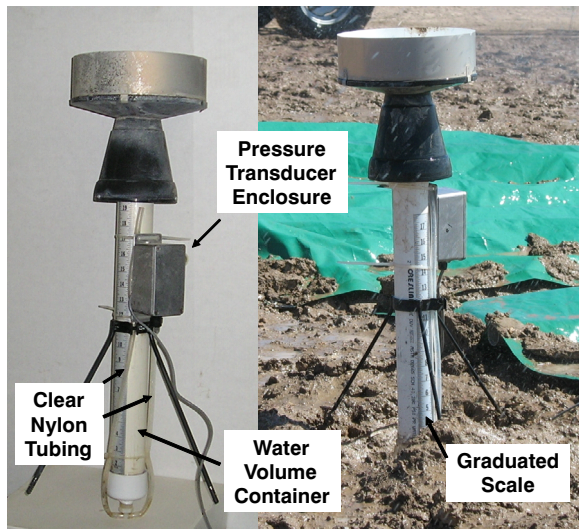
Figure 1. Picture of collector depicting components and typical field installation in a shallow hole to reduce overall height.

volume container was used to calibrate the pressure sensor and account for potential calibration drift between field tests.

The analog output from the piezo-resistive pressure sensor was a differential voltage rather than a ground referenced voltage. The high voltage side of the differential analog output from the pressure sensor was greater than +5V, which prevented direct connection to a CR21X data logger (Campbell Scientific, Inc., Logan, Utah), because input voltage was limited to ±5V. To overcome this issue a differential voltage amplifier circuit was constructed as shown in figure. 2. The differential amplifier circuit was a precision, low-power instrumentation amplifier IC (INA118, Burr-Brown Corp., Tucson, Ariz.) that required a voltage regulator (L7809ABV, STMicroelectonics, Geneva, Switzerland) and a voltage inverter (ICL7660CPA, Intersil Corp., Milpitas, Calif.). The differential amplifier circuit provided a gain of 6 to the analog signal from the piezo-resistive pressure sensor. This amplification increased the nominal output resolution to 0.23 mm/mV (0.09 in./mV). Output from the differential amplifier circuit was recorded using the CR21X data logger. Supply voltage to the amplifier circuit and pressure sensor was provided by the data logger. Supply voltage was also recorded and used to ratiometrically
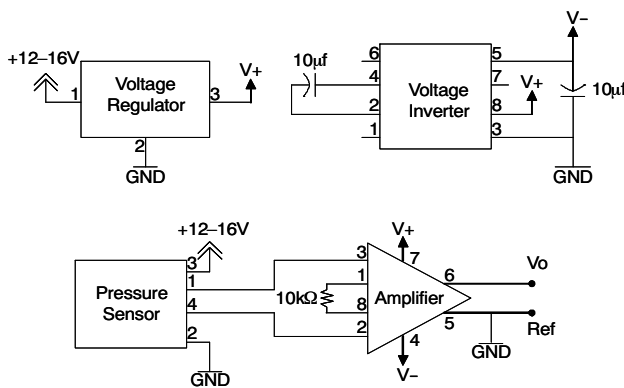

Figure 2. Schematic of differential voltage amplifier circuit used to interfacepiezo-resistive pressure sensor to data logger.

adjust measured output voltage to a reference voltage of 13 VDC. Analog output from the amplifier circuit was measured every second and a running average was computed every second and logged every 15 s.

Functionality of collector design was tested in the laboratory using a variable speed peristaltic pump to fill the water volume container at equivalent application rates ranging from 15 to 204 mm/h (0.6 to 8.0 in./h) while recording output from the differential amplifier. Eleven laboratory tests were performed over the desired range in application rates. Three of the collectors were field tested using a 4-wheel commercial irrigation boom 50 m (164 ft) in length (Briggs Irrigation, Northhamptonshire, UK) to simulate center pivot sprinkler irrigation using four common types of center pivot sprinklers. The irrigation boom was modified by increasing the boom height 460 mm (18 in.) and adding additional sprinkler outlets along the boom length to provide a sprinkler height of approximately 760 mm (30 in.) above the top of the collectors and a sprinkler spacing of 2.43 to 2.59 m (96 to 102 in.). A hydraulic cable winch system mounted on the front of a John Deere 1020 tractor was used to mobilize the irrigation boom. Water was supplied to the irrigation boom through a 76-mm (3-in.), 91-m (300-ft) drag hose. Travel speed of the boom was computer controlled at a specified constant rate. Specific details on the irrigation system used to emulate center pivot sprinkler irrigation are provided by King and Bjorneberg (2007).

Sprinklers used to field test the collector were:
- Nelson R3000 with a brown plate (Nelson Irrigation Corp. Walla Walla, Wash.) with a Nelson 138-kPa (20-psi) pressure regulator.
- Nelson R3000 with red plate with a Nelson 138-kPa (20-psi) pressure regulator.
- Nelson S3000 with purple plate with a Nelson 103-kPa (15-psi) pressure regulator.
- Senninger I-Wob with standard 9-groove plate (Senninger Irrigation Inc., Clermont, Fla.) with a Senninger 103-kPa (15-psi) pressure regulator.
- Nelson D3000 with flat plate with a Nelson 103-kPa (15-psi) pressure regulator.
- Nelson PC3000 part circle with turquoise plate with a Nelson 103-kPa (15-psi) pressure regulator.

Two application rates, high and low, were used to test the collectors under sprinklers 1 though 4. The Nelson D3000 sprinkler was only tested at the high application rate. The high application rate was selected to be representative of that found under the outer end of a 400-m (1100-ft) center pivot sprinkler irrigation system. Sprinkler nozzle sizes were selected to provide approximately the same flow rate for each sprinkler at high and low application rates (based on manufacturers' data) regardless of operating pressure or manufacturer. The selected sprinkler nozzle sizes and corresponding flow rates are listed in table 1. The ability of the collector to detect a steep gradient in application rate was tested using two Nelson PC3000 sprinklers installed in parallel, the high flow rate sprinkler discharging in the direction of irrigation lateral travel and the low flow rate sprinkler discharging in the opposite direction. The flow rate ratio of the PC3000 sprinklers was 3:1 to provide a 3:1 ratio in water application ahead to behind the irrigation lateral. The PC3000 sprinklers with equal application rates ahead and behind the irrigation lateral were also tested. The nozzle

Table 1. Operational data on sprinklers used in field tests of collector.

Sprinkler	Pressure Regulator (kPa)	Application Rate	Nozzle Size (mm)	Flow Rate[a] (L/min)
Nelson R3000	138	High	7.54	42.69
Brown plate	138	Low	5.36	21.23
Nelson R3000	138	High	7.54	42.69
Red plate	138	Low	5.36	21.23
Nelson S3000	103	High	8.14	43.45
Purple plate	103	Low	5.75	21.42
Senninger I-Wob	103	High	8.33	43.00
Standard plate	103	Low	5.56	19.83
Nelson D3000	103	High	8.14	43.45
Flat plate				
Nelson PC3000	103	High	7.14	32.74
Turquoise plate	103	Medium	5.75	21.42
	103	Low	4.17	11.01

[a] Based on manufacturer's data.

sizes and flow rates used are also listed in table 1. Application depths ranged from 13 to 28 mm (0.6 to 1.1 in.).

Radial application rate distributions for the sprinklers used in the field tests were determined by indoor testing. The indoor tests used one of each sprinkler type and associated pressure regulator mounted at a height of 1 m (3.3 ft). Catch cans 150 mm (6 in.) in diameter and 180 mm (7 in.) tall spaced at 0.6-m (2-ft) increments from the sprinkler in one radial direction were used to collect water. The duration of each test was 30 to 60 min. Water collected in each can was measured using a graduated cylinder. Application rate was calculated based on the diameter of the catch cans and duration of the each test. These radial application rate distributions were used to simulate application rate profiles occurring in the field when sprinkler patterns overlap.

RESULTS AND DISCUSSION

LABORATORY TESTS

Cumulative application depth curves measured in laboratory tests of the collector are shown in figure 3. Linear regression analysis was conducted on the cumulative application depth curves to obtain a minimum sum of squared error estimate of application rate (slope) for each test. The resulting application rates are listed in table 2. The regression analysis R^2 exceeded 0.99 for all 11 laboratory tests. The maximum difference between the actual application rate and regression slope was 1.0 mm/h (0.04 in./h) demonstrating that the collector functions as designed.

Application rate under a center pivot irrigation system is not constant so regression analysis cannot be used to determine application rate for field tests, rather numerical differentiation of some form has to be used. Numerical differentiation is a "noisy" operation by amplifying the high frequency discontinuities (dividing by small time increment) as shown in figure 4 for a five-point central difference of the 76.1-mm/h (3.0-in./h) laboratory test (fig. 3). Numerical differentiation of the sampled analog output causes the computed application rate to vary from 64 to 86 mm/h (2.5 to 3.4 in./h) due to noise generated by the pressure sensor, differential amplifier, wiring, and sampling by the data logger. To reduce the presence of random electrical noise, low pass digital filtering was applied to differentiation similar to that used by Ruthroff and Bodtmann (1976) and Tattelman and Knight (1988) to reduce noise in digitized rain gauge data. A digital differentiating filter was designed to reduce the influence of random electrical noise on calculation of application rate. Background on implementation and design of the digital differentiating filter are provided in the Appendix.

Application rates determined using the digital differentiating filter on the cumulative application depth
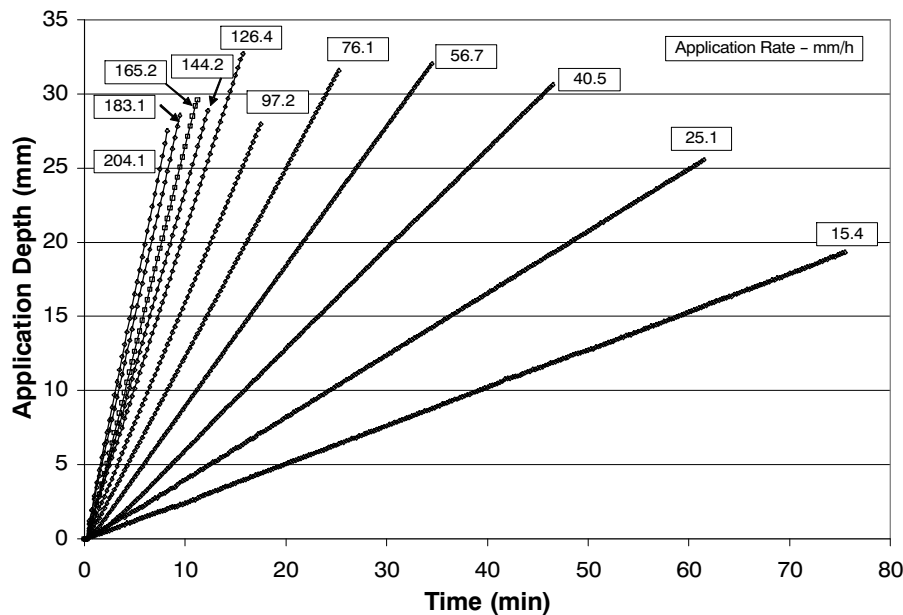

Figure 3. Cumulative application depth curves obtained in laboratory tests of the collector.

Table 2. Comparison of actual application rates in laboratory tests with application rates determined by regression slope of cumulative depth curve and digital differentiating filtering.

Actual Application Rate (mm/h)	Application Rate by Regression Slope		Application Rate by Digital Differentiating Filter	
	(mm/h)	(% difference)	(mm/h)	(% difference)
15.4	15.4	0.0	15.4	0.0
25.1	25.1	0.0	25.0	-0.4
40.5	40.5	0.0	39.7	-2.0
56.7	56.7	0.0	56.1	-1.0
76.1	76.1	0.0	75.8	-0.4
97.2	97.1	0.0	97.2	-0.1
126.4	126.2	0.0	126.9	0.4
144.2	143.8	0.4	144.3	0.7
165.2	164.2	0.6	166.7	0.9
183.1	182.8	0.0	185.2	1.1
204.1	203.4	0.3	206.2	1.0

curves from laboratory tests of the collector are shown in figure 5. Comparison of digital differentiating filtering with a five-point central difference is shown in figure 4 for the laboratory test with 76.1-mm/h (3.0-in./h) application rate. Average application rates computed using the differential digital filter for the laboratory tests are listed in table 2. The maximum difference from the actual rate is 2.1 mm/h (0.08 in./h) or 1.1%. The difference between the actual application rate and the average determined using the differentiating digital filter increases with application rate. The difference is largely due to the short duration transients present at the beginning of each application rate curve determined using the digital differentiating filter (fig. 5). The transients are an artifact of the digital differentiating filter technique when application rate increases instantaneously. This does not significantly affect data collected under field conditions as the application rate is initially small and increases to a peak near the center pivot sprinkler irrigation system lateral (e.g. fig. 7).

FIELD TESTS

Measured radial application rate profiles for the sprinklers, nozzle sizes, and pressures listed in table 1 are shown in figure 6. The radial application rate profiles were used in a simulation program written in Microsoft Visual Basic (Redmond, Wash.) to model cumulative application rate patterns from overlapping sprinkler profiles along a center pivot sprinkler irrigation lateral. The simulated application rate patterns are compared to those measured by the collector in field tests. Application rates measured by three collectors in a field test of the I-Wob standard plate sprinkler are shown in figure 7. The three collectors were spaced at approximately 3.5-m (11.5-ft) intervals in the direction of travel of the irrigation boom and randomly placed in relation to sprinkler spacing along the center pivot sprinkler lateral. Thus, there can be small differences in measured application rate patterns due to location between sprinklers, interference of the struts attaching the sprinkler
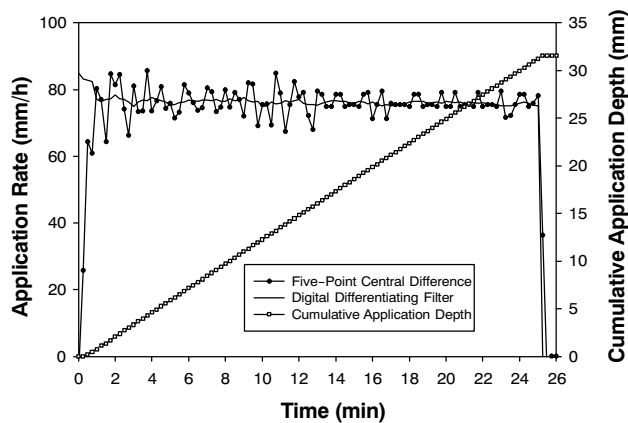

Figure 4. Application rate calculated using five-point central difference and digital differentiating filter for 76.1-mm/h laboratory test.
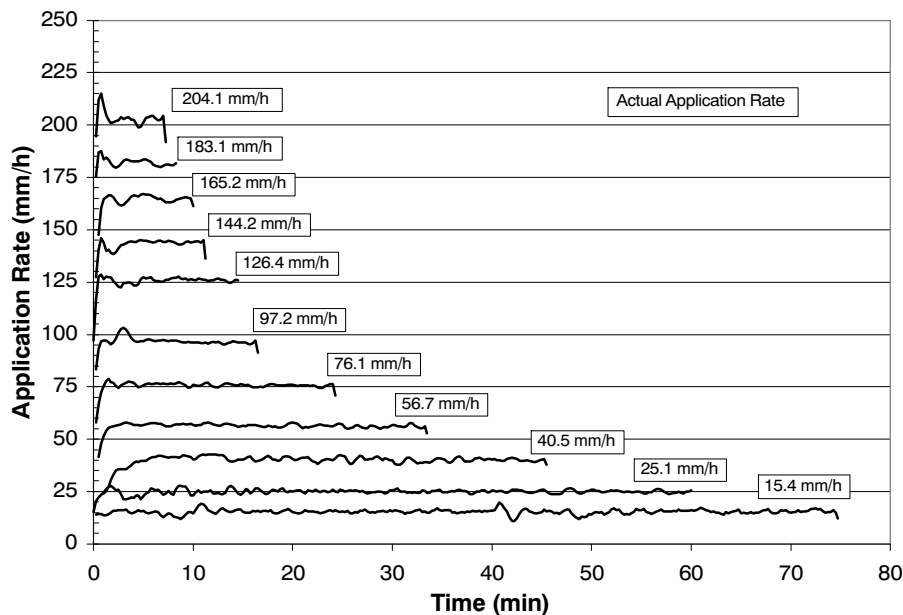

Figure 5. Application rate curves for laboratory tests on the collector calculated using the differential filter.

deflector plate, irrigation system structural interference, and differences in wind speed and direction between sequential collector measurements. All field tests were conducted when wind speed was less than 4.5 m/s (10 mph). Pearson product-moment correlation coefficients (Steele and Torrie, 1980) between the three collector measurements are $r_{12} = 0.87$ between collectors 1 and 2, $r_{13} = 0.97$ between collectors 1 and 3, and $r_{23} = 0.90$ between collectors 2 and 3. Confidence intervals for r using Fisher's Z transform (Steele and Torrie, 1980) show that the response of collector 2 is significantly different (p≤0.01) from collectors 1 and 3. The significant difference is likely due to the measured peak application rate of collector 2 being shifted approximately 2 min relative to collectors 1 and 3. Wind speed was often variable and light during field testing which is likely the cause of the shift in measurements of collector 2 from those of collectors 1 and 3. For the test shown in figure 7, peak 15-min wind gust was 6.3 m/s (14.0 mph) and the 15-min average wind speed was 2.9 m/s (6.6 mph) at the beginning of the test and by the end of the test the peak 15-min wind gust was 3.3 m/s (7.0 mph) and the 15-min average wind speed was 2.0 m/s (4.5 mph). Rain gauge number does not necessarily correspond to the order in which water was applied to the rain gauges.

Average measured application rate patterns for each sprinkler, nozzle size, and pressure listed in table 1 are shown in figures 8, 9, and 10, along with simulated application rate patterns. Pearson correlation coefficients between average measured and simulated application rate patterns for each field test are listed in table 3. Pearson correlation coefficients
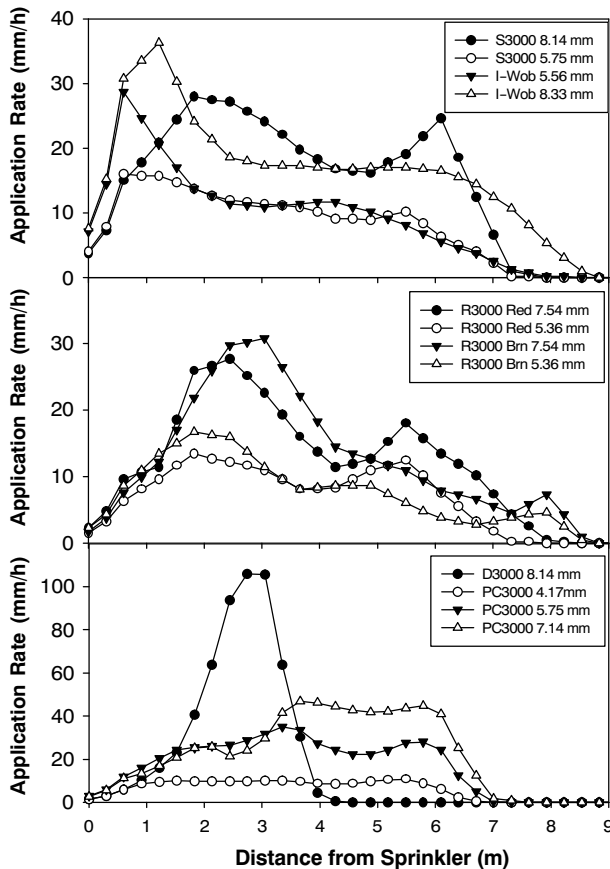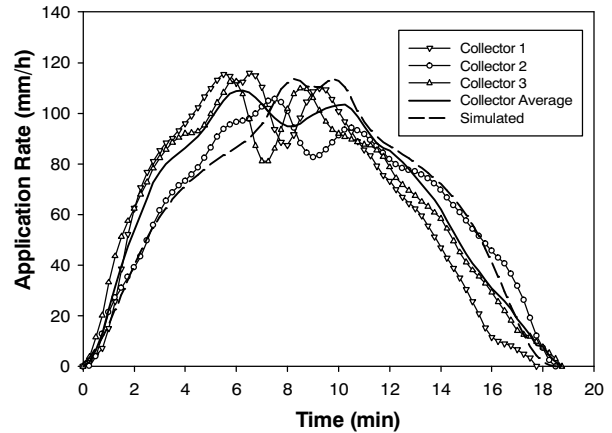

Figure 7. Application rate for I-Wob sprinkler with 8.33-mm nozzle at 138 kPa measured with three collectors compared to average and simulated using sprinkler radial application profile.

were all greater than 0.90 indicating that 81% or more of the collector response is predicted by the simulated application rate pattern. The peak application rate from the collector average application rate pattern is very similar to those calculated using the model of Kincaid (2005) which is based on field data collected under a stationary sprinkler boom using an array of catch cans. Based on a paired t-test of peak application rates, there is no significant difference (p ≤ 0.05) between peak application rates calculated using the model of Kincaid (2005) and those determined from average measured collector application rate patterns. There are greater differences between simulated peak application rates and those determined from average measured collector application rate patterns. The simulation model does not account for wind speed or direction, both of which change under field conditions. Several collector-measured application rates (figs. 8-10) are skewed to the left of the symmetrical simulated application rate pattern. This skew is attributed to a predominant wind direction perpendicular to the sprinkler lateral causing droplet trajectory to vary depending upon whether the droplet travels with or into the wind.

The largest discrepancy between collector-measured and simulated application rate pattern occurs with the skewed PC3000 sprinkler test (fig. 10). The simulation model uses a single sprinkler application rate profile for 180° in the direction of sprinkler lateral travel and a separate application rate profile in the opposing 180° direction. The PC3000 actually has a 190° wetted pattern. Thus, there is overlap of the two application profiles near the sprinkler lateral that is not accounted for by the simulation model. This overlap is the reason for the gradual change in application rate near the sprinkler lateral rather than a sharp change predicted by the simulation model. The reason for the higher peak in the simulation model application rate pattern compared to the collector measure application rate pattern is unknown.

The piezo-resistive pressure sensor used in this study required the use of a differential amplifier to interface the sensor to the data logger. Selection of a more expensive version of a piezo-resistive pressure sensor, which incorporates a voltage regulator and an amplifier with a ground-referenced analog output eliminating the need for an external differential amplifier circuit, is recommended. This may actually reduce overall costs. This may also reduce

Figure 6. Radial application rate profiles for sprinklers used in field testing of collector.
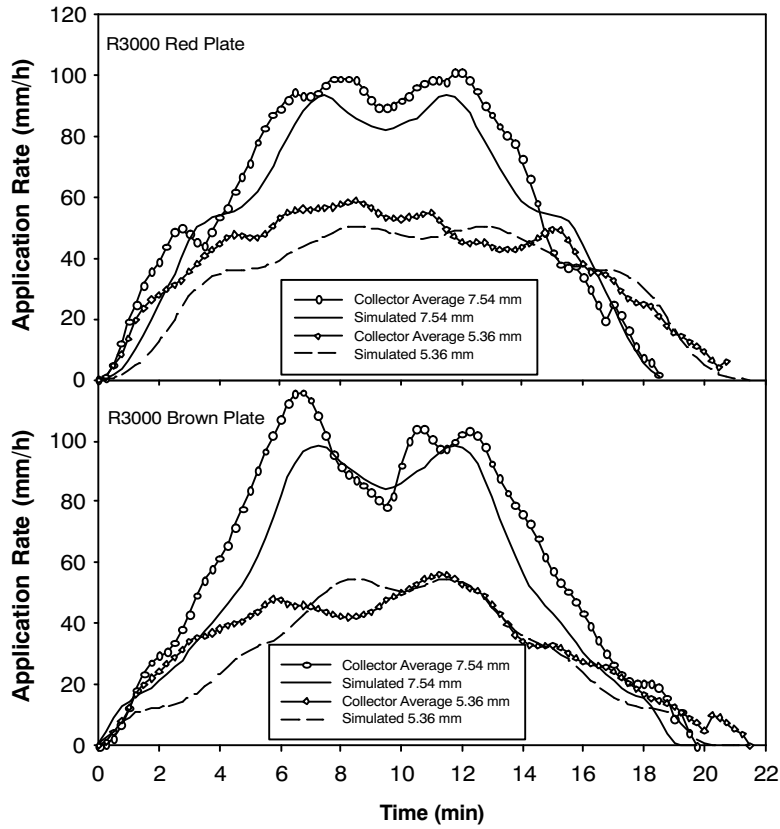
Figure 8. Average application rate for R3000 sprinkler with red and brown plates and with 7.54- and 5.36-mm nozzles at 138 kPa measured with collectors compared to simulated using sprinkler radial application profiles.
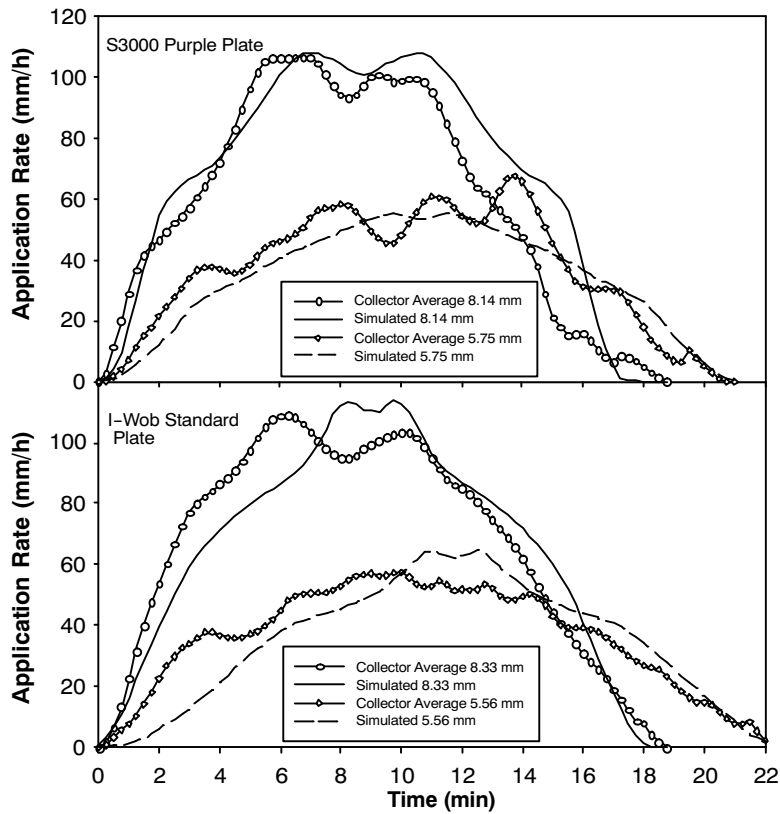

Figure 9. (Top) Average application rate for S3000 sprinkler with purple plate with 8.14- and 5.75-mm nozzles at 108 kPa measured with collectors compared to simulated using sprinkler radial application profiles. (Bottom) Average application rate for I-Wob sprinkler with standard plate with 8.33- and 5.56-mm nozzles at 108 kPa measured with collectors compared to simulated using sprinkler radial application profiles.
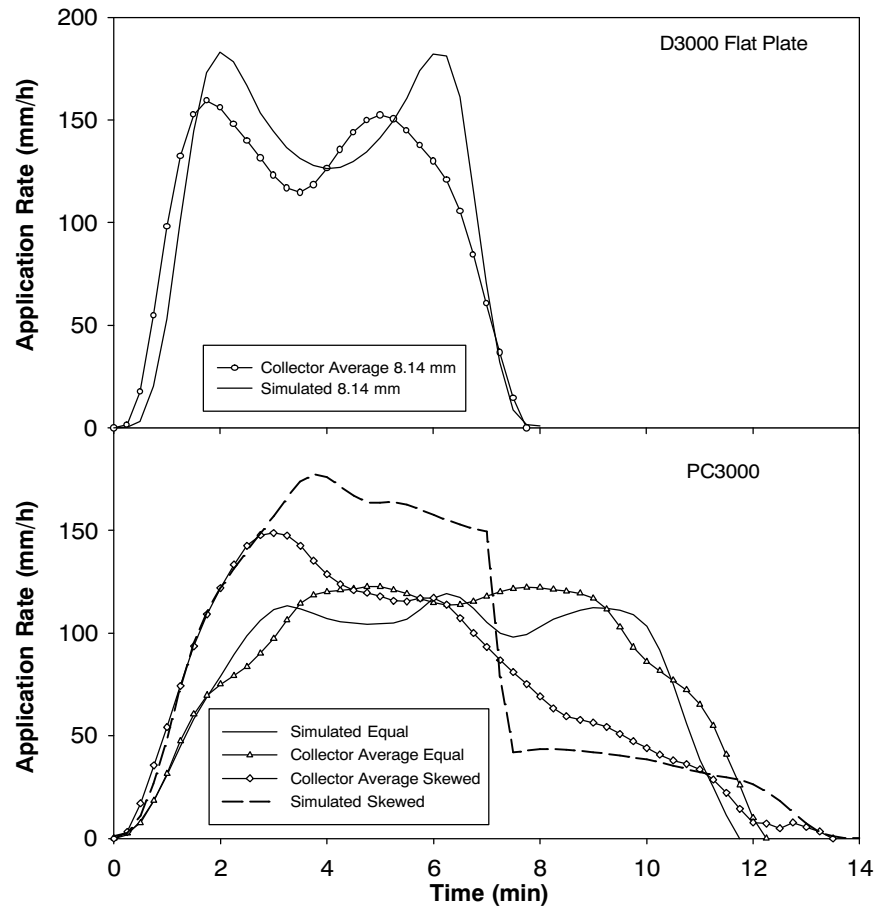
Figure 10. (Top) Average application rate for D3000 sprinkler with flat plate and 8.14-mm nozzles at 108 kPa measured with collectors compared to simulated using sprinkler radial application profiles. (Bottom) Average application rate for PC3000 sprinkler with equal and skewed application pattern measured with collectors compared to simulated using sprinkler radial application profiles.

Table 3. Pearson correlation coefficient between average measured application rate pattern and simulated application rate pattern for each field test. Comparison of simulated and measured peak application rate with that predicted by Kincaid (2005) model.

Sprinkler	Application Rate	Pearson Correlation Coefficient	Simulated	Average Measured	Kincaid (2005) Model
			Peak Application Rate (mm/h)		
R3000	High	0.97	98	116	107
Brown plate	Low	0.93	54	56	57
R3000	High	0.97	94	111	104
Red plate	Low	0.92	50	59	57
S3000	High	0.94	108	107	112
Purple plate	Low	0.94	56	61	64
I-Wob	High	0.94	114	109	109
Standard plate	Low	0.90	65	57	55
D3000	High	0.92	183	159	–
Flat plate					
PCS3000	Equal	0.94	122	119	–
Turquoise plate	Skewed	0.94	177	149	–

the random noise in the analog output and eliminate the need to filter the computed derivative of the analog output used to compute application rate, especially if the sensor includes some signal conditioning with the amplifier. A piezo-resistive sensor with the voltage regulator and amplifier housed in water proof package would be advantageous as moisture condensation in the splash proof enclosure used in this study resulted in sensor failure on several occasions over three years of use.

SUMMARY

A collector was designed to measure time variant high-intensity sprinkler application rates under field conditions. The collector design was tested in the laboratory and under field conditions simulating center pivot sprinkler irrigation. A digital differentiating filter was designed and used to reduce the effect of random electrical noise in the sensor and amplifier output on calculated application rate. For a range in application rates from 15 to 200 mm/h (0.7 to 8 in./h) in the laboratory, the maximum collector error was 2.1 mm/h (0.08 in./h). Collector-measured application rate patterns under field conditions were well correlated to simulated application rate patterns using radial application rate profiles for the sprinklers tested. Collector-measured peak application rates were not significantly different from those predicted by the Kincaid (2005) model. The collector

functioned as designed in field tests and provides an effective and efficient means of measuring high-intensity application rates from center pivot irrigation systems under field conditions.

REFERENCES

Allen, R. G. 1990. Applicator selection along center-pivots using soil infiltration parameters. In *Visions of the Future*, 549-555. St. Joseph, Mich.: ASAE.

Cunningham, E. P. 1992. *Digital Filtering: An Introduction*. Boston, Mass.: Haughton Mifflin.

Dillion, R. C., E. A. Hiler, and G. Vittetoe. 1972. Center-pivot sprinkler design based on intake characteristics. *Trans. ASAE* 15(5): 996-1001.

Gilley, J. R. 1984. Suitability of reduced pressure center-pivots. *Irrig. and Drainage Eng.* 111(1): 22-34.

DeBoer, D. W. 2001. Sprinkler application pattern shape and surface runoff. *Trans. ASAE* 44(5): 1217-1220.

DeBoer, D. W., A. Moshef-Javadi, and S. T. Chu. 1988. Application of the Green-Ampt infiltration equation to sprinkler irrigation management. *Applied Agric. Res.* 3(3): 128-132.

DeBoer, D. W., D. L. Beck, and A. R. Bender. 1992. A field evaluation of low, medium and high pressure sprinklers. *Trans. ASAE* 35(4): 1185-1189.

Habib, E., W. F. Krajewski, and A. Kruger. 2001. Sampling errors of tipping-bucket rain gauge measurements. *J. Hydrol. Eng.* 6(2): 159-166.

Humphrey, M. D., J. D. Istok, J. Y. Lee, J. A. Hevesi, and A. L. Flint. 1997. A new method for automated dynamic calibration of tipping-bucket rain gauges. *J. Atmospheric and Oceanic Tech.* 14(6): 1513-1519.

Kincaid, D. C. 2005. Application rates from center pivot irrigation with current sprinkler types. *Applied Eng. in Agric.* 21(4): 605-610.

Kincaid, D. C., B. A. King, and D. W. DeBoer. 2000. Sprinkler packages and their configurations for center pivot irrigation. In *Visions of the Future*, 109-114. St. Joseph, Mich.: ASAE.

Kincaid, D. C, D. F. Heermann, and E. G. Kruse. 1969. Application rates and runoff in center-pivot irrigation. *Trans. ASAE* 12(6): 790-794,797.

King, B. A., and D. L. Bjorneberg. 2007. Center pivot simulator for evaluating system design and management effects on infiltration and erosion. In *Proc. 28 th Intl. Irrigation Show*. Falls Church, Va.: Irrigation Association.

Oppenheim, A. V., and R. W. Shaffer. 1975. *Digital Signal Processing*. Englewood Cliffs, N.J.: Prentice Hall.

Ruthroff, C. L., and W. F. Bodtmann. 1976. Computing derivatives from equally spaced data. *J. Applied Meteorology* 15(11): 1152-1159.

Sadler, E. J., and W. J. Busscher. 1989. High-intensity rainfall rate determination from tipping-bucket rain gauge data. *Agron. J.* 81: 930-934.

Scherer, T. F., and J. K. Weigel. 1995. Field measurement of the application rate and uniformity of center pivot irrigation systems. ASAE Paper No. SD 95104. St. Joseph, Mich.: ASAE.

Steel, R. G. D., and J. H. Torrie. 1980. *Principles and Procedures of Statistics*. New York, N.Y.: McGraw-Hill.

Tattelman, P., and R. W. Knight. 1988. Analysis of 1-min rain rates extracted from weighing raingage recordings. *J. Applied Meteorology* 27(8): 928-938.

USDA. 2009. 2007 census of agriculture: farm and ranch survey (2008). USDA National Agricultural Statistics Service, Volume 3 Special Studies Part1 AC-07-SS-1. Washington, D.C.

Wang, J., B. L. Fisher, and D. B. Wolff. 2008. Estimating rain rates from tipping-bucket rain gauge measurements. *J. Atmospheric and Oceanic Tech.* 25(1): 43-56.

Wilmes, G. J., D. L. Martin, and R. J. Supalla. 1993. Decision support system for design of center pivots. *Trans. ASAE* 37(1): 165-175.

APPENDIX

DIGITAL DIFFERENTIATING FILTER DESIGN

Fourier series analysis allows an arbitrary periodic signal in the time domain, $f(t)$, to be represented by a DC (zero frequency) component and an infinite series of sine waves of varying amplitude and phase. If the signal is not periodic but of finite time duration, then the signal can be treated as though it is a periodic signal with a period equal to the length of the signal. This relationship is expressed by equations A1 and A2.

$$f(t) = \sum_{n=-\infty}^{+\infty} c_n e^{j\omega_n + \phi} \qquad (A1)$$

where $\omega n = 2\pi f_n$, f_n is the nth frequency component in the series (Hz), and

$$c_n e^{j\omega_n + \phi} = c_n \cos(\omega_n \tau + \phi)$$

or

$$c_n e^{j\omega_n + \phi} = a_n \cos(\omega_n \tau) + j b_n \sin(\omega_n \tau) \qquad (A2)$$

where $j=\sqrt{-1}$, φ is the phase shift (radians) and τ is time (s) and c_n, a_n, and b_n are coefficients.

The derivative of $f(t)$ (eq. A1) is given by equation A3.

$$\frac{d(f(t))}{dt} = jw_n \sum_{n=-\infty}^{+\infty} c_n e^{j\omega_n + \phi} \qquad (A3)$$

Equation A3 shows that taking the derivative of $f(t)$ is equivalent to using an amplifier whose gain increases linearly with frequency (w_n) and asserts a constant 90° phase shift (equivalent to multiplying by the imaginary operator, $j=\sqrt{-1}$). Equation A3 also shows that the constant (DC) is removed because ω_n is zero for n equal to zero. Thus, any constant bias (voltage) in $f(t)$ is removed.

Digital filters represent a collection of algorithms that are designed to select some particular characteristics of a sampled data signal on the basis of the frequency content of the signal. The design methods for low pass, band pass and high pass digital filters are well documented (Cunningham, 1992). A generalized digital filter has the form of equation A4 where $Y(z)$ is the output and $X(z)$ is the input and z is the complex operator, $e^{j\omega T}$, that is the discrete time equivalent to the continuous time operator $s = j\omega$ and T is the sample interval in seconds. The filter order refers to the highest power of z inverse in equation A4. The filter order also determines the number of input and possibly output terms that must be processed by the filter algorithm. For equation A4, J is the order of the numerator polynomial, K is the order of the denominator polynomial, and b_j and a_k are weighting coefficients.

$$Y(z) = X(z) \sum_{j=0}^{J-1} b_j z^{-j} - Y(z) \sum_{k=1}^{K-1} a_k z^{-k} \qquad (A4)$$

Equation A4 can be used to express the general form of a non-recursive or finite impulse response (FIR) filter by setting $a_k = 0$ for all k>0.

Equation A4 is expressed in time domain as shown in equation A5 when each sample instant produces a new output, y[n], that is derived from a weighted sum of a sequence of present and past inputs, x[n-j], as well as a sum of weighted sum of past outputs, y[n-k]. The weighting coefficients, b_j and a_k expressed in equation A4 are identical to those expressed in equation A5. Hence the z inverse operator (z^{-1}) raised to a specific power in (A4) represents a delay in the sequence of inputs and outputs.

$$y[n] = \sum_{j=0}^{J-1} b_j x[n-j] - \sum_{k=1}^{K-1} a_k y[n-k] \qquad (A5)$$

The FIR filter ($a_k = 0$ for k = 0, 1 ,2, … K-1) was selected for this study because it is unconditionally stable and the filter phase shift is linearly proportional to frequency. The latter property allows post processed data to be aligned with preprocessed data by simply shifting one of the data sets by a fixed time value.

The process of differentiating $f(t)$ inherently amplifies high frequency signals (eq. A3) producing distortion in the resulting data set due to the effect of aliasing of sampled signals that contain random noise with high frequency content. Typically, the data from these types of signals are passed though a low pass filter to smooth the data after differentiating. Since noise is generally broadband in nature some of the noise content cannot be removed based upon frequency filtering alone. The challenge is to properly select the low pass cutoff frequency above which the frequency content of the signal is removed. Many times, selecting the cutoff frequency is a qualitative assessment of the resulting filtered signal. Filter design involves determining the specific coefficients for the filter algorithm of equation A4 ($a_k = 0$) based on the data signal characteristics and desired output.

Low-pass digital differentiating filters are designed to approximate the derivative function expressed by equation A3 over a restricted frequency range by careful selection of the b_j coefficients of equation A4. The specific values of the coefficients for a differentiating filter of order 2M+1 are determined using equation A6 (Cunningham, 1992).

$$H(z) = \frac{1}{2} \sum_{n=1}^{M} b_n (z^{n-M} - z^{-n-M}) \qquad (A6)$$

where

$$b_n = -2 \left(\frac{\cos \pi n}{n} \right) \text{for } 1 \leq n \leq M \qquad (A7)$$

and H(z) is the z domain transfer function of the filter. In general, H(z) equals Y(z)/X(z) (The output divided by the input). A first order differentiating filter is comparable to a first order central difference numerical algorithm. Using filters for differentiating that are better approximations with wider bandwidths requires higher order filters that also have longer startup transients.

Digital filters have a group delay equal to one-half the order of the filter. For non-causal data, which includes filtering non-real time signals, the filter group delay can be removed by the application of equation A8 with R equal to the filter order (Cunningham, 1992).

$$Y(z)_{shifted} = z^{\frac{R-1}{2}} \cdot Y(z) \qquad (A8)$$

Digital filters also have startup transients until sufficient data is being processed by the filter algorithm to generate valid outputs. Modifying the filter coefficients using a Kaiser Window function is one method of reducing digital filter startup transients and improving the approximation of differentiating function without adding computational complexity (Oppenheim and Shaffer, 1975). The coefficients of the FIR differentiating filter used in this study were computed using the Kaiser Window function given by equations A9 though A11.

$$b_{MOD}(z) = \sum_{j=0}^{J-1} \left(wind_j \cdot b_j(z) \right)^{-j} \qquad (A9)$$

$$wind_j = \frac{I_o \left(\beta \left(1 - \left(\frac{j - \alpha}{\alpha} \right)^2 \right)^{\frac{1}{2}} \right)}{I_o(\beta)} \qquad (A10)$$

where b_{mod} is the modified z domain polynomial, α and β are filter design parameters, and I_o is a zero order modified Bessel function of the first kind expressed by the infinite sequence of equation A11 that usually converges for N<10.

$$I_o = 1 + \frac{(\beta/2)^2}{(1!)^2} + \frac{(\beta/2)4}{(2!)^2} + \frac{(\beta/2)^6}{(3!)^2} + K + \frac{(\beta/2)^{2N}}{(N!)^2}$$
$$= 1 + \sum_{n=1}^{N} \left(\frac{(\beta/2)n}{(n!)^2} \right) \qquad (A11)$$

The design parameter α is the order of the original differentiating filter divided by two and β is the term that determines the cutoff frequency as well as the quality of derivative function approximation within the pass band. The order of the filter used in this study was 5 or $\alpha = 2.5$ based on sample field data analysis (not shown).

The steps required to apply digital differentiating filtering to cumulative application depth data from the collector is illustrated in figure A1. The steps for computing application rate from the time series cumulative application depth data is to process the application depth data with the differentiating filter followed by passing the output from the differentiating filter though a low pass filter. The application rate data from the differentiating filter AR_f (eq. 1) is validated by shifting the filtered data to realign it with the original cumulative application depth data and performing discrete integration using equation A12 to compute a filtered cumulative application depth D_f [mm, (in.)]. The absolute difference, AD [mm (in.)], is then computed using equation A13 where N is equal to the number of data samples in the cumulative application depth data.
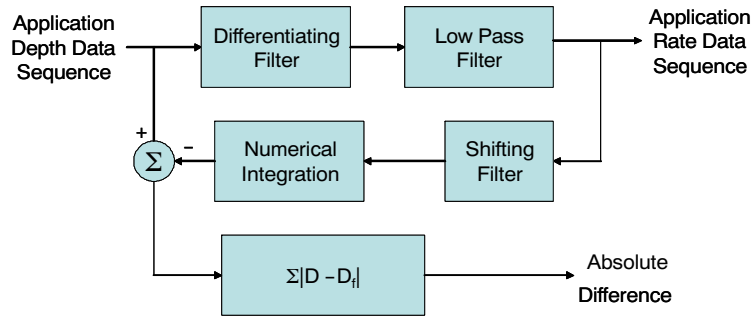
Figure A1. Block diagram of steps required to apply differentiating filter to cumulative application depth data from collector to determine application rate.

$$D_{f_n} = \sum_{m=0}^{n} AR_m \text{ for } 0 \leq n \leq N - 1 \qquad (A12)$$

$$AD = \sum_{n=0}^{N-1} \left| D_n - D_{f_n} \right| \qquad (A13)$$

Determining the specific design of low pass and differentiating digital FIR filters is a subjective process requiring analysis of the dynamics of the system, the data noise characteristics, and the frequency range of information that is to be gleaned by the processing. If the bandwidth chosen is too wide, then the desired information will be distorted by measurement and process noise. If the bandwidth used is too narrow, then the desired system dynamics can be removed.

The band limited differentiating digital filter design parameter, β, was selected using trial and error to minimize the sum of absolute differences expressed by equation A12. Figure A2 demonstrates the effect selection of β has on computed cumulative application depth and application rate. Although the two differentiating filtered application rates shown in figure A2 appear very similar, the differences between computed cumulative application depth is readily apparent. The computed cumulative application depth curve for β = 9.15 in figure A2 is coincident with the collector-measured application depth. The high degree of correlation is a result of data shifting using equation A8. For the case where the differentiating filter was designed with β = 5, the AD computed by equation A11 is 25.0 mm (1.0 in.). When the differentiating filter is designed with β = 9.15, the AD is 4.7 mm (0.2 in.). All analysis of collector data in this study used β = 9.15 as this was the optimum value for sample field data and considered constant for the measurement system. The digital differentiating filter algorithms were implemented in Mathcad (ver. 13, Parametric Technology Corp., Needham, Mass.) and used to process the analog data from the collectors.
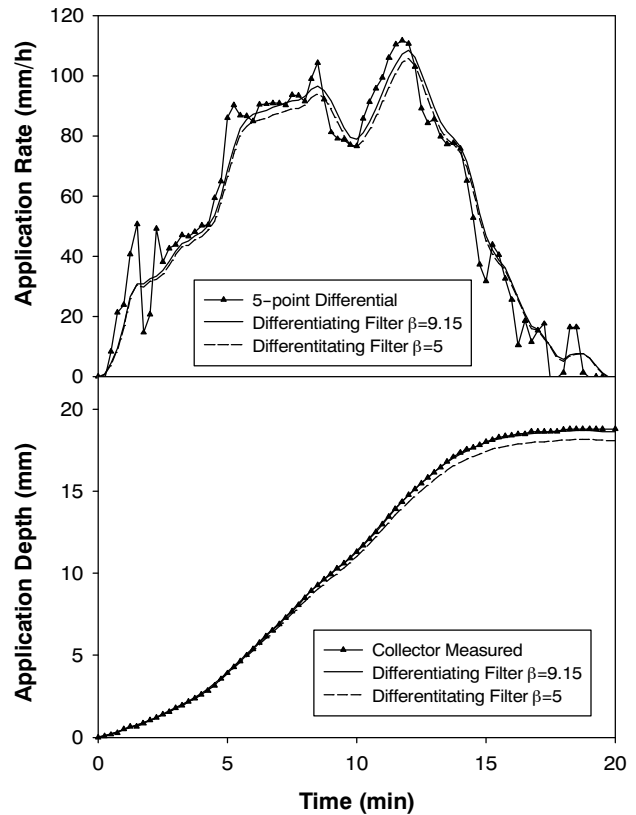

Figure A2. Effect differentiating filter design parameter β has on calculated application rate compared to five-point central differentiation and calculated application depth compared to collector-measured volume.